Proceedings of the Combustion Institute 41 (2025) 105833

Contents lists available at ScienceDirect

Proceedings of the Combustion Institute

journal homepage: www.elsevier.com/locate/proci

Detailed Modeling of Flame-Wall-Interactions under the influence of phosphorous-containing Flame Retardants and development of a reduced kinetic model

Vanessa Stegmayer *, Ulrich Maas, Christina Strassacker

Karlsruhe Institute of Technology, Institute of Technical Thermodynamics, Engelbert-Arndold-Strasse 4, Karlsruhe 76131, Germany

ARTICLE INFO

Keywords:
Flame-wall interaction
Flame retardants
REDIM
Reduced kinetic models
DMMP

ABSTRACT

Fire safety engineering plays a vital role in safeguarding lives, property, and the environment by preventing and mitigating fire hazards in buildings, materials, and systems. Phosphorus-based flame retardants, such as dimethyl methylphosphonate (DMMP), are studied for their effectiveness in inhibiting combustion processes. This study investigates the impact of flame retardants on Flame-Wall Interactions by adding varying amounts of DMMP to a premixed methane/air Head-On Quenching flame, where the flame propagates towards a cold wall and extinguishes. Reduced kinetic models for these systems with different DMMP concentrations are developed using the Reaction-Diffusion Manifold (REDIM) method. The REDIM is constructed and validated by comparing results of detailed and reduced kinetics. In this way, the quality of the REDIM reduced kinetics can be verified for the different phenomena resulting due to the inhibiting character of flame retardants. It is shown that the reduced kinetics reproduce the results of the Flame-Wall Interactions under the influence of flame retardants very accurately. The inhibiting character of the flame retardants with respect to the chemical kinetics is well captured, even though it challenges the generation of the reduced kinetics as the amount of added DMMP is very low and in the magnitude of minor species. Additionally, the sensitivity of the simulation with reduced kinetics on the gradient estimate is investigated, showing little to no sensitivity. This model offers significant potential for fire safety engineering, as the drastic reduction in the number of equations enables the analysis of realistic scenarios facilitating the design of safer systems.

1. Introduction

Flame retardants are very important in fire safety engineering, as they reduce the risk of ignition, cause quenching, and slow the spread of fire in materials and products [1–3]. Their influence on flame propagation is, therefore, investigated both numerically [4–8] and experimentally [5,7–9] and models to describe combustion systems under the influence of flame retardants have been developed.

In order to numerically investigate systems including flame retardants, detailed mechanisms have been developed that accurately describe the influence of inhibiting compounds in flames [4,9–11]. These mechanisms can be used to investigate the influence of flame retardants in different configurations, e.g. extinction processes close to cold walls. These so-called Flame-Wall Interactions (FWI) have been investigated in a number of works without flame retardants (e.g. [12,13]) and recently also with the addition of flame retardants [8,11]. However, complex chemical kinetics lead to very time-consuming simulations due to the large number of species and the vast differences in time scales that lead to high stiffness of the partial differential equation system [14,15]. One way to overcome this problem is the use of reduced kinetic models [14,15]. Manifold-based models are often used due to their low dimensionality and high accuracy compared to the simulations with detailed kinetics (detailed chemical mechanism). Different reduced kinetic models have been developed and implemented (e.g. [16–20], an overview is given in [14,21]) varying in their level of complexity and accuracy. There are reduced kinetic models accounting only for the chemical kinetics (e.g. Intrinsic Low Dimensional Manifold [19], Method of Invariant Manifold [22], Global Quasi Linearization [23] or Quasi Equilibrium Manifold [24]) or accounting for chemical kinetics and molecular transport processes (e.g. Flamelet Generated Manifold [16,17] and Reaction Diffusion Manifold (REDIM) [20]). Due to consideration of molecular transport processes, the latter reduced models are more accurate and are able to better predict crucial processes, e.g. the extinction in presence of flame retardants or in turbulent combustion regimes [25]. Previous studies examined wall extinction [12,

* Corresponding author.
E-mail address: vanessa.stegmayer@kit.edu (V. Stegmayer).

https://doi.org/10.1016/j.proci.2025.105833
Received 7 May 2025; Accepted 2 September 2025
Available online 18 September 2025

26], but to the authors' knowledge no reduced kinetic models exist for flame-retardant effects.

This work investigates FWI under the influence of phosphorus-containing flame retardants and derives a reduced kinetic model for extinction processes including flame retardants. Flame retardants inhibit the chemical kinetics, resulting in a different extinction behavior, which challenges the generation of the reduced kinetics, which should reproduce the detailed kinetics with as high accuracy as possible. For the generation of the reduced kinetic model, the REDIM method is used, which incorporates both chemical kinetics and transport processes, allowing it to handle phenomena such as extinction. A detailed transport model including thermal diffusion is used to model the transport processes [27]. In this work a detailed chemical kinetic mechanism is used that includes flame-inhibiting species and reactions, and appropriate reduced kinetic models are generated for different amounts of DMMP. These reduced kinetic models will be implemented and validated to demonstrate the accuracy of REDIM reduced kinetics.

2. Definition of the model system

In order to analyze FWI with flame retardants and demonstrate REDIM for extinction with inhibiting compounds, a model system consisting of a premixed methane/air flame that travels towards a cold wall, where heat losses cause quenching, is used. This configuration is refereed to as Head-On Quenching (HOQ). In order to study the influence of flame retardants, Dimethyl methylphosphonate (DMMP) is added to the premixed gas mixture. The mole fraction of DMMP in the unburned mixture, ranges from $x_{DMMP} = 0$ to 0.0125, resulting in different extinction behaviors. This range was chosen because the effectiveness of DMMP is reduced with increasing volume fraction and the change in system behavior becomes very small [5,6,28]. Due to the symmetry and the assumption that a large diameter burner is modeled, only one spatial coordinate – the coordinate perpendicular to the wall – is needed to describe the system numerically. Therefore, the one-dimensional reacting flow solver INSFLA [29] can be used for the numerical integration.

The model system consists of a one-dimensional flame traveling towards a cold wall, located at r = 0 m in the computational domain, which has a constant temperature of $T_W = 500$ K.[1] Therefore, a Dirichlet boundary condition is applied for the temperature. For the species diffusion fluxes at both boundaries as well as the temperature at the boundary away from the wall, zero gradients are applied. The temperature of the unburnt gas is T = 500 K and the pressure is considered to be constant at $p = 1$ bar. A schematic of the system can be found in the supplemental material.

In order to model the chemical kinetics, a mechanism provided by Jayaweera et al. [10] is used. The mechanism has been shown to have a good agreement in the range used, without being too complex. The method can, however be applied to other mechanisms. For the description of the diffusion processes, a detailed transport model based on the Curtiss-Hirschfelder approximation [30] is used. Depending on the added amount of DMMP, different evolutions and extinction behaviors of the detailed description are observed. The following methodology demonstrates how the REDIM method can model these different extinction processes.

[1] This temperature reflects the conditions relevant to a flame retardant project within a collaborative research center, where a temperature of 500 K is used as benchmark because a polymer matrix with flame retardants, which are released during polymer melting, is used.

3. FWI with flame retardants

3.1. Reaction-diffusion manifolds

In order to calculate the evolution of a reacting system, the system of evolution equations for reacting flows Eq. (1) needs to be solved where the state vector reads $\boldsymbol{\psi} = \left(h, p, \frac{w_1}{M_1}, \ldots, \frac{w_n}{M_n}\right)$ with enthalpy h, pressure p, mass fractions w_n and molar masses M_n of all n species. Moreover, $\boldsymbol{v}$ represents the velocity field, $\mathbf{F}$ the source term, ρ the density and $\mathbf{D}$ the matrix of the transport coefficients. $\boldsymbol{\phi}(\boldsymbol{\psi})$ represents the vector field.

$$\frac{\partial \boldsymbol{\psi}}{\partial t} = \mathbf{F} - \boldsymbol{v}\,\mathrm{grad}\boldsymbol{\psi} + \frac{1}{\rho}\mathrm{div}\left(\mathbf{D}\cdot\mathrm{grad}\boldsymbol{\psi}\right) \equiv \boldsymbol{\phi}(\boldsymbol{\psi}) \tag{1}$$

The REDIM method is a reduced kinetic model that accounts for both chemical reaction and molecular transport. Since the system involves drastically different time scales both the chemical source term and the transport term cause the existence of low-dimensional manifolds. The REDIM method assumes that only a few reactive and diffusive processes couple [31]. The fast and very slow chemical time scales can be decoupled and the slow scales are coupled to the transport processes. The states during combustion processes are constrained to a low dimensional manifold. These manifolds can be parameterized by a small number of variables, m, represented by the vector $\boldsymbol{\theta} = (\theta_1, \ldots, \theta_m)$ of generalized coordinates, which represent the local coordinates on the manifold. The state vector can be expressed as a function of these generalized coordinates, where $m \ll n+2$ and is given as $\boldsymbol{\psi} = \boldsymbol{\psi}(\boldsymbol{\theta})$. As a result, the number of dimensions of the manifold defines the number of coordinates that are needed to determine the state vector. It is assumed that the system solution is close to or belongs to the invariant manifold defined by $\boldsymbol{\psi}(\boldsymbol{\theta}) \to \boldsymbol{\theta}$

$$M = \{\boldsymbol{\psi} : \boldsymbol{\psi} = \boldsymbol{\psi}(\boldsymbol{\theta}), \boldsymbol{\psi} : R^m \to R^n\}. \tag{2}$$

For each point on the manifold the invariance condition $\left(\boldsymbol{\psi}_\theta^\perp(\boldsymbol{\theta})\right)^T \cdot \boldsymbol{\phi}(\boldsymbol{\psi}) \equiv 0$ applies [20]. Here, $\boldsymbol{\psi}_\theta^\perp$ defines the normal space to the manifold and $\boldsymbol{\phi}(\boldsymbol{\psi})$ the vector field. This invariance condition states that the vector field for points on the manifold is normal to the manifold.

The low dimensional manifold is identified by applying a projection operator $\mathbf{P} = \mathbf{I} - \boldsymbol{\psi}_\theta \boldsymbol{\psi}_\theta^+$ to the evolution equation. Here $\boldsymbol{\psi}_\theta^+$ is the Moore–Penrose Pseudo-Inverse of the derivative of $\boldsymbol{\psi}$ with respect to $\boldsymbol{\theta}$. Due to this projection, the convective term cancels out and the REDIM equation is given by [20]

$$\frac{\partial \boldsymbol{\psi}}{\partial t} = \left(\mathbf{I} - \boldsymbol{\psi}_\theta \boldsymbol{\psi}_\theta^+\right)\left(\mathbf{F} + \frac{1}{\rho}\left(\mathbf{D}\cdot\boldsymbol{\psi}_\theta \chi\right)_\theta \chi\right) \tag{3}$$

This equation is independent of parametrization $\boldsymbol{\theta}$. The gradient estimate χ, which defines the molecular transport processes on the REDIM and is part of the diffusion term of the REDIM equation, which estimates both the size and the time scales of the physical processes and thus reflects the coupling between chemical reaction and diffusion, needs to be provided. In order to solve this equation, an initial guess needs to be specified for every generated REDIM. This initial guess serves as a starting solution of the REDIM integration process. After integration of this equation the found REDIM is used in a reduced computation to validate the reduced model.

3.2. Specification of the initial guess

The initial guess and especially its boundaries need to be constructed in a way that makes it possible to account for the heat loss as well as for the chemical kinetics in the considered system. Therefore, manifold based reduced kinetic models are usually parameterized by two dimensions, with the specific enthalpy describing the heat loss towards the wall and a progress variable for the species describing the progress of chemical reaction [12,13]. In order to obtain the initial guesses of the manifold, detailed sample solutions of the model system are taken and grids for the different amounts of DMMP are generated.

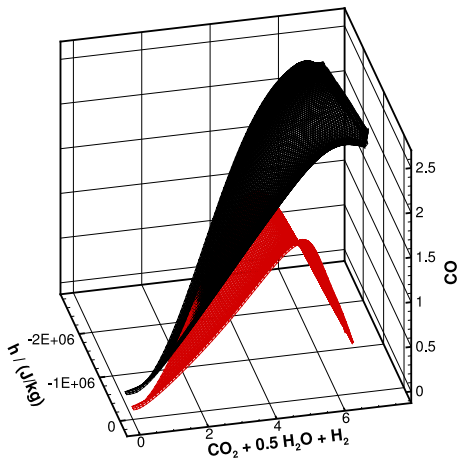

Fig. 1. REDIMs of the stoichiometric flame without flame retardants (red mesh) and of the stoichiometric flame with added DMMP (mole fraction $x_{DMMP} = 0.0125$, black mesh) in the state space. The species are given in mol/kg and the specific enthalpy h in J/kg.

For a unique parametrization of these grids, the specific enthalpy as well as the linear combination $CO_2 + 0.5 \cdot H_2O + H_2$ are used, describing the heat loss to the wall and the progress of the chemical kinetics. The parametrization variable is used merely for a suitable parametrization of the manifold. The manifold itself does not depend on the parametrization and is not influenced by the initial guess.

3.3. Specification of the gradient estimation

The gradient estimate χ can be taken either from detailed sample solutions or can be guessed. In this work, the gradient estimate of the physical variables is obtained from detailed sample solutions of the model system. The gradients are then transformed into gradients of generalized coordinates via $\chi = \mathrm{grad}(\theta) = \boldsymbol{\psi}_\theta^+ \mathrm{grad}(\boldsymbol{\psi})$.

The REDIM equation is solved starting from the initial guesses using the provided gradient estimates. The stationary solution ($t \to \infty$) provides the REDIM. At this point the invariance condition is fulfilled and $\left(\mathbf{I} - \boldsymbol{\psi}_\theta \boldsymbol{\psi}_\theta^+\right) \cdot \boldsymbol{\phi}(\boldsymbol{\psi}) = 0$ applies. The results are then stored in REDIM tables that can be used in subsequent simulations [20]. Fig. 1 shows as an example the REDIMs for the system without added DMMP and for $x_{DMMP} = 0.0125$ in the state space. The addition of DMMP leads to different assessed states due to the inhibiting character of phosphorous compounds (see e.g. [32,33]). Note, that these states coincide with the results of the detailed kinetics.

In order to investigate the sensitivity of the reduced calculation/REDIM on the gradient estimate different gradient estimations are used to generate various REDIMs. The gradient estimate determined from the detailed sample solution is varied by a factor α.

$$\mathrm{grad}\boldsymbol{\psi} = \alpha \cdot \mathrm{grad}\boldsymbol{\psi}_{det.} \tag{4}$$

The REDIM evolution equation is then integrated for the different gradient estimates resulting in different REDIMs, which are then used for calculations with reduced kinetics.

3.4. Implementation of REDIM reduced kinetics

For the validation of the generated reduced kinetic models, the integrated REDIMs are used for computations with the same initial conditions as for the computations with detailed kinetics. Afterwards, the results of reduced and detailed kinetics are compared to each other in order to determine the accuracy of the reduced model. For the implementation of the REDIMs, the reduced model equation in generalized coordinates is used. The advantage of this implementation strategy is that the system dynamics is projected onto the tangential subspace of the manifold, compensating small defects in the invariance of the manifolds. The model equation for the temporal evolution of the generalized coordinates is derived by multiplying both sides of eq. (1) with $\boldsymbol{\psi}_\theta^+$ yielding

$$\frac{\partial \boldsymbol{\theta}}{\partial t} = \boldsymbol{\psi}_\theta^+ \mathbf{F} + \boldsymbol{v}\mathrm{grad}\boldsymbol{\theta} + \frac{1}{\rho}\boldsymbol{\psi}_\theta^+ \mathrm{div}\left(\mathbf{D} \cdot \boldsymbol{\psi}_\theta \mathrm{grad}\boldsymbol{\theta}\right). \tag{5}$$

$\boldsymbol{\psi}_\theta^+ \mathbf{F}$, $\boldsymbol{\psi}_\theta^+(\boldsymbol{\theta})$ and $\mathbf{D} \cdot \boldsymbol{\psi}_\theta$ are taken from the REDIM-tables [20]. The boundary conditions at the wall for the species and temperature is analogous to the detailed kinetics given by $\frac{\partial j}{\partial x}\left(\boldsymbol{\theta}(r_W)\right) = 0$ and $T\left(\boldsymbol{\theta}(r_W)\right) = T_W$. Here $\boldsymbol{j}$ is the vector of diffusion flux densities. On the right side of the domain, zero gradients are applied for all state variables. Eq. (5) is implemented in INSFLA and the partial differential equations are solved for the different model systems (different amounts of DMMP) for $\boldsymbol{\theta} = (\theta_1, \theta_2)$. Therefore, the dimension of the system is reduced and the computational time is reduced to around $1/35$ of the computational time of the detailed kinetics.

4. Results

To study FWI under the influence of flame retardants, calculations of the HOQ process are performed with different amounts of DMMP. Fig. 2 shows the time evolution of these calculations for the detailed and reduced kinetics. The spatial profiles of the temperature and the specific molar number of OH are shown. The flame moves towards the cold wall and quenches there. It can be observed that the temperature of the flat flame with less DMMP is higher and the width of the flame front is smaller, resulting in a higher flame speed [32,34]. The inhibition effect of DMMP on the laminar flame speed is mainly due to the reduction of the OH concentration [6]. The phosphorus chemistry inhibits the flame by recombining the important combustion radicals (e.g. H and OH) with phosphorus-containing species, e.g. to PO_2, HOPO and $HOPO_2$ (see [32,33]). This can be observed by the different amounts of OH.

Both figures show good agreement of the reduced kinetics with the detailed kinetics and that the inhibiting character of phosphorus compounds can be modeled with the REDIM reduced kinetics for the proposed HOQ process.

The heat flux density to the wall – an important quantity for the extinction processes at walls – is investigated in order to compare the results of the reduced kinetics with those of the detailed kinetics. The heat flux density towards the wall $q_{wall} = |-\lambda \mathrm{grad}T|$ and its temporal evolution, as shown in Fig. 3, allow a comparison of the flame velocities as well as a comparison of the maximum gradients of temperature and heat transfer. Both the time of maximum heat flux density and the magnitude of the maximum heat flux density are characteristic values for the description of quenching processes at walls. The maximum of the heat flux density to the wall indicates the heat transferred to the wall, which is influenced by, among other things, the flame thickness, which is also changed by the addition of DMMP. A good agreement of the time of the maximum heat flux density of the detailed and reduced kinetics indicates that the flame velocity is reproduced correctly by the reduced kinetic model. Fig. 3 shows that both the amount of the maximum heat flux density as well as the time of the maximum heat flux density are reproduced very well by the reduced kinetics for all different amounts of added DMMP. Therefore, the flame velocity as well as the flame thickness are reproduced very well by the reduced kinetics.

In order to investigate the extinction behavior in more detail, the states at the time of quenching are examined. The time of quenching is defined by the time of maximum heat flux density to the wall of each calculation. Fig. 4 shows the spatial profiles of the temperature T as well as the spatial profiles of the specific mole numbers of the species H, CH_4 and CO for the mole fractions $x_{DMMP} = 0$ and $x_{DMMP} = 0.0107$ at the time of quenching. The spatial temperature profile changes

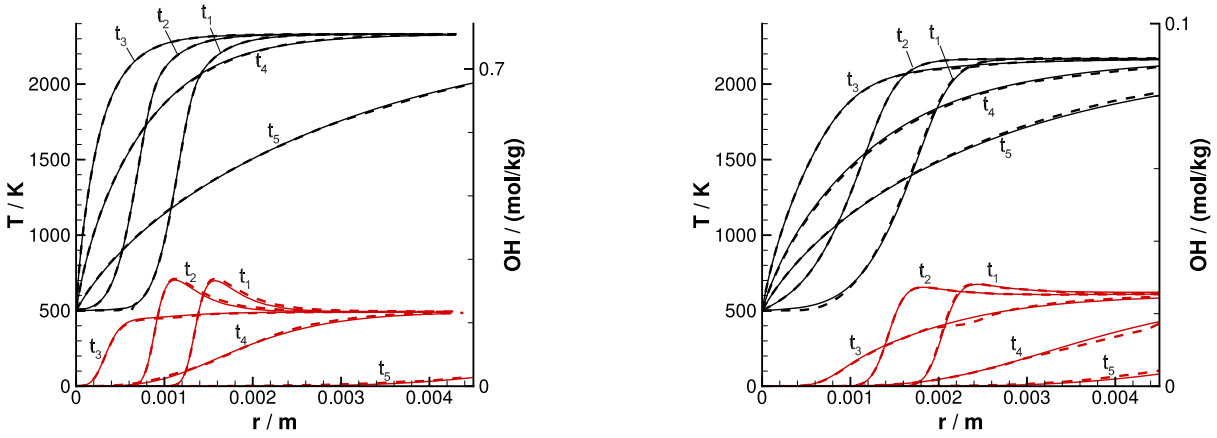

(a) $x_{DMMP} = 0.0018$ (b) $x_{DMMP} = 0.0107$

Fig. 2. Evolution of the spatial profiles ($t_1 < t_2 < t_3 < t_4 < t_5$) of the temperature (black) and the specific mole numbers of OH (red). Illustrated are the computations with detailed kinetics (solid lines) and reduced kinetics (dashed lines) with different mole fractions x_{DMMP} of added flame retardant.

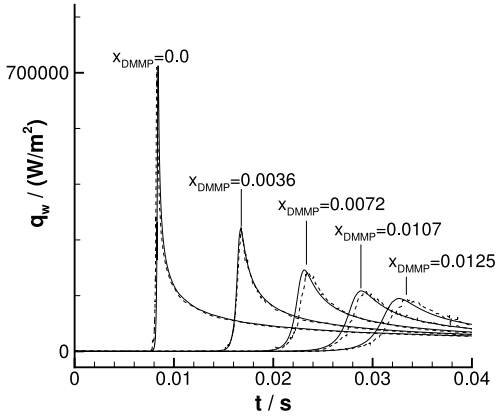

Fig. 3. Heat flux density towards the wall (in W/m^2) as a function of the time t (in s) for the detailed kinetics (solid lines) and reduced kinetics (dashed lines) with different mole fractions x_{DMMP} of added flame retardant.

with increasing DMMP. The maximum flame temperature for the mole fraction $x_{DMMP} = 0.0036$ is slightly higher than for the calculation without added DMMP. The reason for this is the higher enthalpy of formation of P – O bonds compared to C – O bonds, therefore DMMP preferentially consumes O_2 resulting in a higher heat release and temperature per amount of O_2 consumed [34,35]. For the calculation with $x_{DMMP} = 0.0107$, the maximum temperature decreases as the flame becomes increasingly inhibited. Furthermore, the spatial profiles of the species differ significantly. As a result, the amount of the specific mole number of H behind the flame front in the burned gas decreases for the calculation without added DMMP, while it increases for all other calculations shown. This means that the H concentration has already reached its equilibrium values within the flame front due to catalytic radical recombination [5]. Moreover, it can be observed that with an increasing mole fraction of DMMP, the amount of remaining CH_4 at the time of quenching increases, the flame front becomes wider and, therefore, the temperature at certain positions in front of the wall at the time of quenching decreases. As a result, less CH_4 is decomposed in front of the wall. However, almost all CH_4 is converted in the burned gas for all calculations. This is different for the spatial profile of the specific mole number of CO. In the calculation without DMMP, the amount of CO decreases constantly in the post-flame zone because it is further oxidized to CO_2. With an increasing amount of DMMP, CO is not completely converted to CO_2 and the amount of remaining CO increases. This observation can also be seen in Fig. 1. The reason for this observation is that the radicals necessary to further oxidize CO are already caught in phosphorous containing particles, e.g. PO_2, HOPO, and $HOPO_2$. The figures show that the REDIM reduced kinetics reproduce the detailed kinetics at the time of quenching very well and there are only minor discrepancies between the results. It is again demonstrated that the REDIM reacts on the small changes of added DMMP and correctly reproduces the system dynamics.

For the purpose of comparing the actual quenching behavior in more detail, the quenching distance is investigated. In this work, the quenching distance is determined by measuring the maximum value of CH_3 at the time of quenching, which is defined by the time of maximum heat flux density to the wall for the different calculations. The species CH_3 is chosen for this investigation because it has a maximum within the flame front for all investigated calculations. Fig. 5 shows the quenching distance for the detailed as well as for the reduced kinetics. An approximately linear relation between the molar ratio of DMMP and the measured quenching distance can be observed. As a result of the decreasing flame speed with increasing DMMP the spacial profiles of the flame front become wider and as a result the quenching distance increases. In addition, the spatial gradients of the state variables with increasing amount of DMMP decrease and transport processes (e.g. heat conduction and diffusion of radicals) become slower leading to larger quenching distances. It can be seen that the reduced kinetics reproduce the quenching distance of the detailed kinetics very well.

In order to further study the temporal evolution of the extinction process, the states at the distance $r_W = 0.4$ mm in front of the wall are investigated. At this position, a significant influence of the wall on the flame is given for all different computations. Fig. 6 shows the comparison for different species as a function of the specific mole number of CO_2 – an indicator for the progress of combustion – is suitable to demonstrate the processes of extinction. As can be observed, the amount of produced CO_2 decreases constantly for increasing DMMP-ratios. The maximum amount of produced CO strongly depends on the amount of DMMP, as shown in the graph for CO. For little added DMMP, less maximum CO is produced compared to the calculation without DMMP but the CO is not completely consumed again after the flame is quenched. This is caused by two competing processes: the flame inhibition by the phosphorous compounds leading to less produced CO, and no further oxidation of CO to CO_2. Further increasing the amount of DMMP increases the amount of produced CO and for $x_{DMMP} = 0.0125$, CO is not consumed at all after the quenching process. The species C_2H_2 is exemplarily illustrated for minor species. Here, the produced C_2H_2 is consumed after the flame front traveled by at r_W and the flame is extinguished. Moreover, it can be observed that the

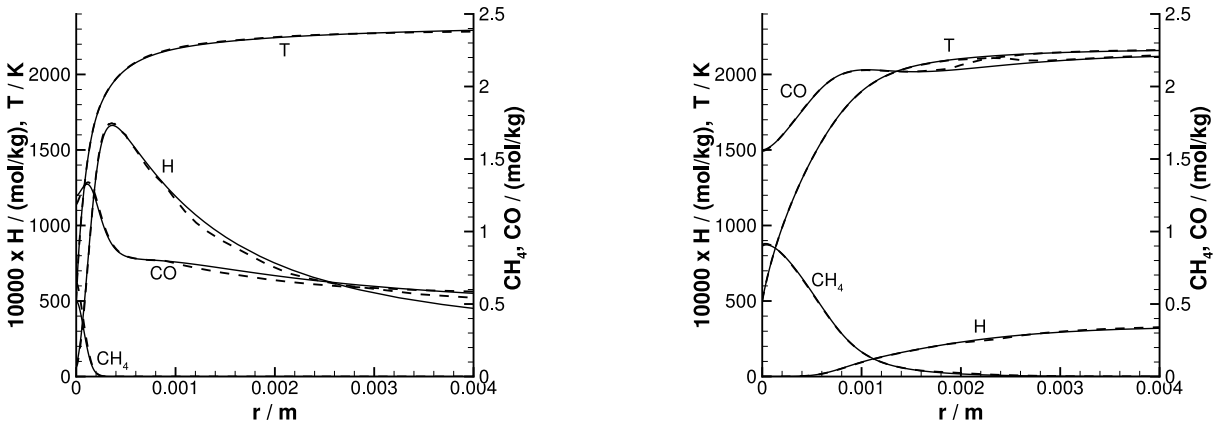

Fig. 4. Spatial profiles of the specific mole numbers of CO, H and CH_4, (in mol/kg) as well as the temperature T at the time of quenching. Illustrated are the computations with detailed kinetics (solid lines) and reduced kinetics (dashed lines) with different mole fractions x_{DMMP} of added flame retardant.

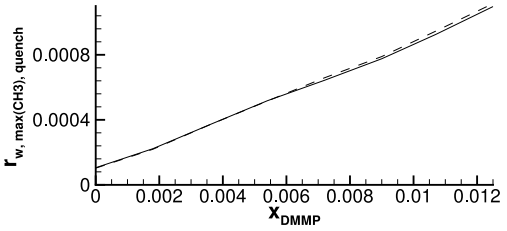

Fig. 5. Location of the maximum value of CH_3 at the time of quenching (indicated by the maximum heat flux density) (in m) as a function of the molar ratio of DMMP.

produced C_2H_2 increases with increasing amount of DMMP. Usually, in an uninhibited flame, C_2H_2 is consumed in reactions with e.g. O, OH or H, which are, due to the phosphorous compounds, already bond to other molecules. Therefore, less C_2H_2 is consumed and the amount increases with increasing mole fraction of added DMMP. The evolution of a phosphorous compound is also shown. The maximum amount of HPO_2 is observed for an intermediate amount of DMMP. After the flame is quenched, HPO_2 is partially consumed and decreases. Regarding the validation of the REDIM it can be seen that the reduced kinetics reproduce the evolution of the detailed kinetics very well for all different species with and without phosphor. This demonstrates that the REDIM reduced kinetics are able to recapture the extinction process very accurately, even under the influence of added flame retardants. In order to show how the sensitivity of the detailed mechanism is reflected by the reduced calculation a sensitivity study investigating some reactions from the DMMP sub-mechanism is shown in the supplemental material.

For the sensitivity analysis, the reduced simulation in which the gradient estimate is derived directly from the detailed calculation is compared to the reduced simulation where the gradient estimate is increased by a factor α. Fig. 7 shows the heat flux density towards the wall for different variations of the gradient estimate for $x_{DMMP} = 0.0018$ and $x_{DMMP} = 0.0107$. The heat flux density for $x_{DMMP} = 0.0018$ shows good agreement for all α, as its deviation for the maximum heat flux density does not exceed 10% compared to the heat flux density for $\alpha = 1$. A similar observation can be made for $x_{DMMP} = 0.0107$. While the simulation for $\alpha = 0.5$ fits the one for $\alpha = 1.0$ very well, the one for $\alpha = 1.5$ is sightly higher and $\alpha = 2.0$ shows an increase of approximately 8%. The fluctuations in the graph result from changes in the gradients during the adaptive grid refinement. The fluctuations occur due to the static grid adaption. Using more grid points or fixing the grid point distance to the wall would lower these fluctuations. Furthermore, it can be observed that the time of the maximum heat flux density changes with α. This is more apparent for $x_{DMMP} = 0.0107$. As α increases, the maximum heat density occurs earlier. For $\alpha = 0.5$ the opposite is the case. It also needs to be noted that this change in time is bigger for increasing α. This is because the flame speed is higher for bigger α resulting in earlier times of quenching. The increased flame speed for larger α is evident from the initial flame propagation, as the flame is already delayed at the beginning, far from the wall. The shift in time of maximum heat flux is more significant at higher DMMP concentrations. Hence, it can be concluded that the simulation is more sensitive with respect to the gradient estimate for higher amounts of DMMP, though the overall agreement remains good. The same applies to the flame velocity and the flame thickness.

5. Conclusion

In the present work, Flame-Wall Interactions under the influence of flame retardants were investigated. DMMP was added at different amounts to a premixed flame quenching at a cold wall. For modeling the chemical kinetics, a detailed mechanism including phosphorus compounds was used to model the complex kinetics of the influence of DMMP on the flame [10]. In addition, reduced kinetic models were generated to allow time-efficient simulations of flame-wall interactions with flame retardants. The REDIM method was used for model reduction and validated by comparing the results of detailed and reduced kinetics. The sensitivity to gradient estimation was also investigated.

It is shown that the transient system behavior of the considered model configuration can be reproduced very well. There is a good agreement of the corresponding reduced and detailed kinetics for the different amounts of DMMP added for the investigations in the state space, heat flux density and quenching distance. The influence of DMMP and the system dynamics can therefore be reproduced accurately using the REDIM method. It is also shown, that the reduced model is not sensitive on the gradient estimate. Additionally, the use of REDIM reduced kinetics reduced the computational time by a factor of 35 compared to detailed kinetics. As two-dimensional REDIM for HOQ can be used in further studies to investigate Side-Wall Quenching, without noticeable loss of accuracy the REDIM method provides not only savings in computational time for HOQ but also for other applications [36].

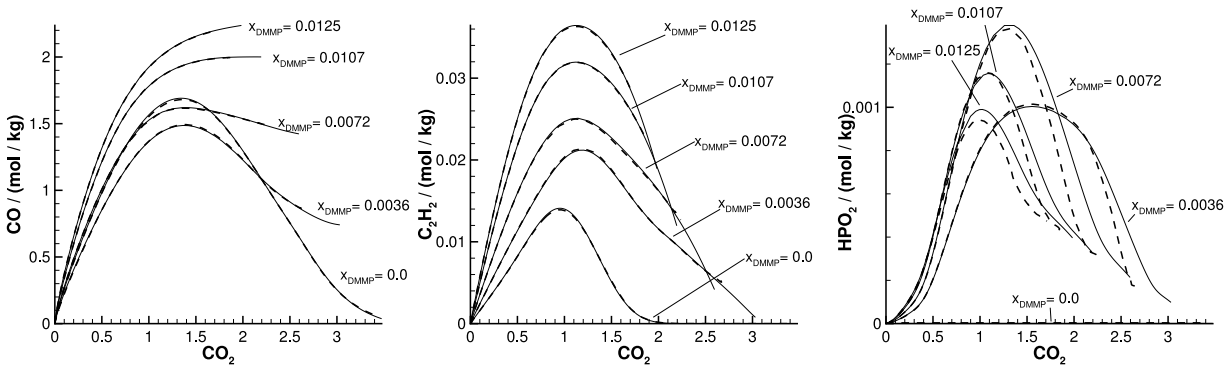

Fig. 6. Specific mole numbers of CO, C_2H_2 and HPO_2 (in mol/kg) as a function of the specific mole number of CO_2 at the position r = 0.0004 m in front of the wall. Illustrated are the computations with detailed kinetics (solid lines) and reduced kinetics (dashed lines) with different mole fractions x_{DMMP} of added flame retardant.

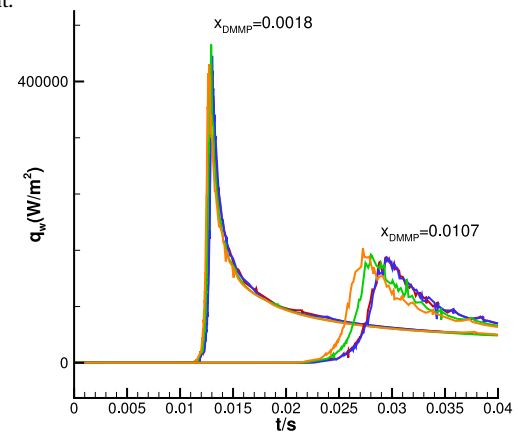

Fig. 7. Heat flux density towards the wall (in W/m^2) as a function of the time t (in s) for different gradient estimates $\text{grad}\psi_{det.}$ (red) and $\text{grad}\psi = \alpha \cdot \text{grad}\psi_{det.}$ with $\alpha = 0.5$ (blue), $\alpha = 1.5$ (green) and $\alpha = 2.0$ (orange) for $x_{DMMP} = 0.0018$ and $x_{DMMP} = 0.0107$.

Novelty and significance statement

Novelty and significance statement The novelty of this research is the first application of the reaction diffusion manifold method (REDIM) for model reduction for Flame-Wall Interaction (FWI) using phosphorous containing flame retardants. The inhibiting character of the flame retardant with respect to the chemical kinetics is well captured, even though it challenges the generation of the reduced kinetics due to the complexity of the chemical system. It is shown that the REDIM method can be used to accurately reproduce FWI with DMMP, as the transient behavior and the dynamics due to inhibition, are captured well, while also significantly reducing computation time. Therefore, this model can be adopted for fire safety engineering because with this drastic reduction in numbers of equations that need to be solved, realistic cases with complex geometries can be addressed.

CRediT authorship contribution statement

Vanessa Stegmayer: Writing – original draft, Formal analysis, Data curation. **Ulrich Maas:** Writing – review & editing, Supervision, Software. **Christina Strassacker:** Writing – original draft, Software, Formal analysis, Data curation, Conceptualization.

Declaration of competing interest

The authors declare that they have no known competing financial interests or personal relationships that could have appeared to influence the work reported in this paper.

Acknowledgments

This work was funded by the Deutsche Forschungsgemeinschaft (DFG, German Research Foundation) – Projektnummer 237267381 – TRR 150, subproject B06.

Appendix A. Supplementary data

Supplementary material related to this article can be found online at https://doi.org/10.1016/j.proci.2025.105833.

References

[1] M. Zhang, A. Buekens, X. Li, Brominated flame retardants and the formation of dioxins and furans in fires and combustion, J Hazard. Mater. 304 (2016) 26–39.
[2] C. Ma, J. Wang, Y. Yuan, X. Mu, Y. Pan, L. Song, Y. Hu, An insight into gas phase flame retardant mechanisms of AHP versus alpi in PBT: Online pyrolysis vacuum ultraviolet photoionization time-of-flight mass spectrometry, Combust. Flame 209 (2019) 467–477.
[3] G.M. Wu, B. Schartel, H. Bahr, M. Kleemeier, D. Yu, A. Hartwig, Experimental and quantitative assessment of flame retardancy by the shielding effect in layered silicate epoxy nanocomposites, Combust. Flame 159 (12) (2012) 3616–3623.
[4] A. Twarowski, Reduction of a phosphorus oxide and acid reaction set, Combust. Flame 102 (1–2) (1995) 41–54.
[5] N. Bouvet, G.T. Linteris, V.I. Babushok, F. Takahashi, V.R. Katta, R. Krämer, A comparison of the gas-phase fire retardant action of DMMP and Br_2 in co-flow diffusion flame extinguishment, Combust. Flame 169 (2016) 340–348.
[6] N. Bouvet, G. Linteris, V. Babushok, F. Takahashi, V. Katta, R. Krämer, Experimental and numerical investigation of the gas-phase effectiveness of phosphorus compounds, Fire Mater. 40 (2015) 683–696.
[7] A. Shmakov, O. Korobeinichev, V. Shvartsberg, D. Knyazkov, T. Bolshova, I. Rybitskaya, Inhibition of premixed and nonpremixed flames with phosphorus-containing compounds, Proc. Combust. Inst. 30 (2) (2005) 2345–2352.
[8] M. Steinhausen, F. Ferraro, M. Schneider, F. Zentgraf, M. Greifenstein, A. Dreizler, C. Hasse, A. Scholtissek, Effect of flame retardants on side-wall quenching of partially premixed laminar flames, Proc. Combust. Inst. 39 (3) (2023) 3745–3754.
[9] V.I. Babushok, G.T. Linteris, D.R. Burgess Jr., P.T. Baker, Hydrocarbon flame inhibition by $C_3H_2F_3Br$ (2-BTP), Combust. Flame 162 (4) (2015) 1104–1112.
[10] T. Jayaweera, C. Melius, W. Pitz, C. Westbrook, O. Korobeinichev, V. Shvartsberg, A. Shmakov, I. Rybitskaya, H.J. Curran, Flame inhibition by phosphorus-containing compounds over a range of equivalence ratios, Combust. Flame 140 (1–2) (2005) 103–115.
[11] F. Ferraro, A. Stagni, A. Scholtissek, The role of chemistry in the retardant effect of dimethyl methylphosphonate in flame–wall interaction, Proc. Combust. Inst. 40 (1) (2024) 105529.
[12] C. Strassacker, V. Bykov, U. Maas, Reduced modeling of flame-wall-interactions of premixed isooctane-air systems including detailed transport and surface reactions, Proc. Combust. Inst. 38 (1) (2021) 1063–1070.
[13] S. Ganter, C. Straßacker, G. Kuenne, T. Meier, A. Heinrich, U. Maas, J. Janicka, Laminar near-wall combustion: Analysis of tabulated chemistry simulations by means of detailed kinetics, Int. J. Heat Fluid Fl. 70 (2018) 259–270.

[14] D.A. Goussis, U. Maas, Model reduction for combustion chemistry, in: Turbulent Combustion Modeling, Springer, Dordrecht, 2011, pp. 193–220.
[15] J. Warnatz, U. Maas, R.W. Dibble, Physical and Chemical Fundamentals, Modeling and Simulation, Experiments, Pollutant Formation, Springer, Heidelberg, 1990.
[16] J. Van Oijen, L. De Goey, Modelling of premixed laminar flames using flamelet-generated manifolds, Combust. Sci. Technol. 161 (1) (2000) 113–137.
[17] P.-D. Nguyen, L. Vervisch, V. Subramanian, P. Domingo, Multidimensional flamelet-generated manifolds for partially premixed combustion, Combust. Flame 157 (1) (2010) 43–61.
[18] P. Coelho, N. Peters, Unsteady modelling of a piloted methane/air jet flame based on the Eulerian particle flamelet model, Combust. Flame 124 (3) (2001) 444–465.
[19] U. Maas, S.B. Pope, Simplifying chemical kinetics: intrinsic low-dimensional manifolds in composition space, Combust. Flame 88 (3–4) (1992) 239–264.
[20] V. Bykov, U. Maas, The extension of the ILDM concept to reaction–diffusion manifolds, Combust. Theor. Model. 11 (6) (2007) 839–862.
[21] T. Turányi, A.S. Tomlin, Analysis of Kinetic Reaction Mechanisms, vol. 20, Springer, Heidelberg, 2014.
[22] A.N. Gorban, I.V. Karlin, Method of invariant manifold for chemical kinetics, Chem. Eng. Sci. 58 (21) (2003) 4751–4768.
[23] C. Yu, F. Minuzzi, V. Bykov, U. Maas, Methane/air auto-ignition based on global quasi-linearization (GQL) and directed relation graph (DRG): implementation and comparison, Combust. Sci. Technol. 192 (9) (2020) 1802–1824.
[24] A.N. Gorban, I.V. Karlin, Method of invariant manifold for chemical kinetics, Chem. Eng. Sci. 58 (21) (2003) 4751–4768.
[25] C. Yu, X. Li, C. Wu, A. Neagos, U. Maas, Automatic construction of REDIM reduced chemistry with a detailed transport and its application to CH_4 counterflow flames, Energ. Fuel 34 (12) (2020) 16572–16584.
[26] C. Strassacker, V. Bykov, U. Maas, Comparative analysis of reaction-diffusion manifold based reduced models for head-on-and side-wall-quenching flames, Proc. Combust. Inst. 38 (1) (2021) 1025–1032.
[27] J. Warnatz, U.M. und R.W. Dibble, Verbrennung: physikalisch-chemische Grundlagen, Modellierung und Simulation, Experimente, Schadstoffentstehung, third ed. Springer, Berlin, 2001.
[28] V. Babushok, G. Linteris, V. Katta, F. Takahashi, Influence of hydrocarbon moiety of DMMP on flame propagation in lean mixtures, Combust. Flame 171 (2016) 168–172.
[29] U. Maas, J. Warnatz, Ignition processes in hydrogen oxygen mixtures, Combust. Flame 74 (1) (1988) 53–69.
[30] J. De Charentenay, A. Ern, Multicomponent transport impact on turbulent premixed H_2/O_2 flames, Combust. Theor. Model. 6 (3) (2002) 439.
[31] V. Bykov, U. Maas, The extension of the ILDM concept to reaction–diffusion manifolds, Combust. Theor. Model. 11 (6) (2007) 839–862.
[32] T. Sikes, O. Mathieu, W.D. Kulatilaka, M.S. Mannan, E.L. Petersen, Laminar flame speeds of DEMP, DMMP, and TEP added to H_2-and CH_4-air mixtures, Proc. Combust. Inst. 37 (3) (2019) 3775–3781.
[33] A. Twarowski, The influence of phosphorus oxides and acids on the rate of H+ OH recombination, Combust. Flame 94 (1–2) (1993) 91–107.
[34] W. Li, Y. Jiang, Y. Jin, X. Zhu, Investigation of the influence of DMMP on the laminar burning velocity of methane/air premixed flames, Fuel 235 (2019) 1294–1300.
[35] P.A. Sullivan, R. Sumathi, W.H. Green, J.W. Tester, Ab initio modeling of organophosphorus combustion chemistry, Phys. Chem. Chem. Phys. 6 (17) (2004) 4296–4309.
[36] Y. Luo, C. Strassacker, F. Ferraro, F. Zentgraf, A. Dreizler, U. Maas, C. Hasse, A manifold-based reduction method for side-wall quenching considering differential diffusion effects and its application to a laminar lean dimethyl ether flame, Int. J. Heat Fluid Flow 97 (2022) 109042.